

D14.4: Protocol for Characterization of Complete Solar Concentrators Using Photogrammetry or Deflectometry

SFERA II Project	
Solar Facilities for the European Research Area -Second Phase	
Grant agreement number:	312643
Start date of project:	01/01/2014
Duration of project:	48 months
WP14 – Task 14.2	Deliverable 14.4
Due date:	12/2016
Submitted	02/2018
File name:	SFERA-II_D14_4_DLR_170518.docx
Partner responsible	DLR
Person responsible	Christoph Prah (DLR)
Author(s):	Christoph Prah (DLR), Christoph Happich (DLR), Jesús Fernández Reche (CIEMAT),
Dissemination Level	PU



List of content

Executive summary	5
Glossary.....	7
1 Introduction	8
1.1 Motivation	8
1.2 Definition of coordinate system	10
1.3 Measurement quantities	11
2 Measurement methods	16
2.1 Scanning methods	16
2.2 Deflectometry.....	16
2.3 Photogrammetry	19
2.4 Others (not part of the protocol)	19
3 Protocol for characterization of complete solar concentrators with photogrammetry	20
3.1 Points of interest.....	21
3.1.1 Points to be measured on PTC steel structures	21
3.1.1.1 Absorber tube	22
3.1.1.2 Collector longitudinal axis.....	23
3.1.1.3 Water-level.....	23
3.1.1.4 Mirror mounting points	23
3.1.2 Changes in the points to be measured with the reflective collector	24
3.2 Measured quantities and results.....	24
3.2.1 SDX (depending on spatial resolution).....	25
3.2.2 Local angles of the mirror mounting points	25
3.2.3 Deflection by dead load in zenith position	26
3.2.4 Deformation between different operating positions	27
3.3 Tolerances	28
3.4 Equipment.....	29
3.5 Boundary conditions	31
3.6 Preparations	31
3.6.1 General requirements.....	32
3.6.2 Placement of markers on structures.....	33
3.7 Data acquisition	33
3.8 Evaluation and post-processing	35



3.8.1	From images to 3D coordinates	35
3.8.2	Transformation of measured data into the design data coordinate system	35
3.8.3	Additional correction measures	36
3.8.4	Comparison with nominal data and determination of the collector quality	37
3.8.4.1	Aspects for the complete module with attached mirror panels.....	37
3.8.5	Deformation analysis	37
3.9	Data format	38
4	Protocol for characterization of complete solar concentrators with the distant observer method .	39
4.1	Equipment.....	40
4.2	Boundary conditions	40
4.3	Preparations	42
4.3.1	SCE module.....	42
4.3.2	Equipment.....	42
4.3.2.1	Man lift	42
4.3.2.2	Inclinometer mounting	42
4.3.2.3	Camera setup	43
4.3.2.4	Camera calibration.....	44
4.4	Data acquisition	44
4.4.1	Safety issues	44
4.4.2	Position of camera and man –lift	45
4.4.3	Angle range	45
4.4.4	Image acquisition.....	46
4.4.5	Measurement of camera position	46
4.4.6	Absorber tube position.....	46
4.5	Evaluation and post-processing	47
4.5.1	Software.....	47
4.5.2	Determination of 3D setup.....	47
4.5.3	Image rectification.....	48
4.5.4	Detection of absorber tube reflection.....	48
4.6	Calculation of mirror shape.....	49
4.7	Data format.....	49
5	Protocol for characterization of complete solar concentrators with airborne deflectometry.....	51
5.1	Equipment.....	51
5.2	Boundary conditions	52



5.3	Preparation and data acquisition	52
5.4	Evaluation and post-processing	54
6	Measurement of solar concentrators with laser trackers.....	54
6.1	Equipment.....	54
6.2	Boundary conditions	55
6.3	Preparation and data acquisition	55
6.4	Evaluation and post-processing	56
7	References	56



Executive summary

The EU-funded research project - SFERA aims to boost scientific collaboration among the leading European research institutions in solar concentrating systems, offering European research and industry access to the best research and test infrastructures and creating a virtual European laboratory. The project incorporates the following activities:

- **Transnational Access:** Researchers will have access to five state-of-the-art high-flux solar research facilities, unique in Europe and in the world. Access to these facilities will help strengthen the European Research Area by opening installations to European and partner countries' scientists, thereby enhancing cooperation.
- **Networking:** These include the organisation of training courses and schools' to create a common training framework, providing regularised, unified training of young researchers in the capabilities and operation of concentrating solar facilities. Communication activities will seek to both strengthen relationships within the consortium, creating a culture of cooperation, and to communication to society in general, academia and especially industry what SFERA is and what services are offered.
- **The Joint Research Activities** aim to improve the quality and service of the existing infrastructure, extend their services and jointly achieve a common level of high scientific quality.

This Deliverable D14.4 is the results of the WP 14.1 "Characterization of solar concentrators' geometrical quality" and 14.2 "Protocols for characterization of parabolic trough concentrators" within the Joint Research Activities.

The overall objective of WP14 is to define common protocols to be applied at the participating research infrastructures for characterization of solar concentrators.

Deliverable D14.4 aims at providing an overview on latest measurement techniques to qualify the geometry of parabolic trough collectors by means of close range photogrammetry and deflectometry.

Measurement quantities and state-of-the-art approaches are briefly described. The protocol involves a detailed description of the used sensors and equipment, the process of data



acquisition, ambient conditions and the evaluation procedure.

Results of the application of these protocols to parabolic trough concentrators are provided among others in D 14.5 (Round-robin test results).



Glossary

CSP - Concentrating Solar Power	8
DF- Deflectometry	9
DNI- Direct Normal Irradiance	8
DO- Distant Observer	17
IC - Intercept factor	11
PG - Close Range Photogrammetry.....	9
POI – point of interest.....	21
PTC - Parabolic Trough Collectors.....	8
TARMES- Trough Absorber Reflex Measurement System.....	17



1 Introduction

The conversion from solar radiation DNI (Direct Normal Irradiance) to heat and electricity in CSP (Concentrating Solar Power) plants is characterized by the efficiency of a cascade of conversion steps like:

- Concentration and absorption of the solar radiation in the collector
- Heat losses to the environment during transport/storage of the thermal energy in the absorber tubes and header pipes
- Performance of the power block.

The optical performance of the solar field plays a major role for the power plant performance, because any losses at this stage cannot be compensated by subsequent conversion steps. The optical performance is determined by the geometry and optical properties of mirrors, absorber tubes, as well as by the concentrator structure and the tracking systems. In order to determine the optical performance of CSP concentrators, accurate and high resolution data of the concentrator geometry must be obtained. This is commonly done by optical measurement techniques using digital still cameras.

This document provides an overview on state of the art characterization methods for single mirrors and complete solar concentrators, in particular PTCs (Parabolic Trough Collectors). Heliostats are covered in SFERA II D14.7.

The main objective is to provide detailed protocols for the characterization of CSP concentrators, in order to enable other R&D institutions and CSP industry to gain access to this knowledge.

1.1 Motivation

CSP concentrators are high precision and large scale optical devices. Meeting tight tolerances of the geometry is of prime importance to reach the aimed at optical and thermal performance. Thus, the optical, mechanical, and thermal properties of all components of the solar field are crucial for the final efficiency of the power plant.



At all stages from technology development, from prototyping, solar field erection to operation and maintenance, the assessment of the performance of CSP systems and components is an important task and a variety of measurement techniques has been adapted or developed for this purpose. Thermal performance measurements are used to characterize the ability of systems and components to harness incoming irradiation, while minimizing thermal losses to the environment (Janotte, Feckler et al. 2014). Yet, in most cases, the underlying physical effects are not considered in detail.

In view of the geometric characterization, non-contact, optical measures are established approaches. Yet, the optical characterization of large scale CSP concentrators is a demanding topic. The objective is to achieve measurement accuracy in the tenth of *mm*- or *mrad*¹-range for large structures. Data acquisition takes place in the solar field, which involves varying ambient conditions (illumination, wind, and temperature). The collectors are exposed to varying direction of gravitational forces on the structures (tracking), wind forces, and thermal expansion. Measurement equipment is expected to be mobile and compact. The interference with plant operation or construction process shall be as small as possible, so the data acquisition should be fast and there should be least requirements to install additional sensors.

These contradictory requirements and conditions limit the possibilities for the certain measurement approaches. The techniques deflectometry and close range photogrammetry are suitable to fit these requirements and offer complementary characteristics. Both have been deployed by many research groups in the field of CSP concentrator characterization.

The document is structured as follows:

After defining the measurement quantities in Section 1.3, the two measurement approaches Close Range Photogrammetry (PG) and Deflectometry (DF) are presented in detail in Section 2. Section 3 provides the protocol for the characterization of PTCs using PG. The protocol of deflectometric characterization of PTCs is provided in Sec. 4 and 5, respectively. Here, a distinction is made between ground-based or air-borne data-acquisition. Former ground based cameras can be replaced by airborne cameras using Unmanned Aerial Vehicles (UAVs), which greatly enhances measurement volume and degree of automation.

1

1 mrad refers to 1/1000 rad (=0.057°)

The deliverable D14.5 (Round Robin Test) of the SFERA II project presents, among others results, the intercomparison of geometry data from PTC modules derived with PG, DF, and laser scanners

D14.6 focuses on the overall optical thermal and optical characterization of PTCs, which included results from this deliverable. D14.6 also provides information regarding torsion measurements of PTCs, which is a geometrical quantity derived with methods beyond the scope of D 14.4.

1.2 Definition of coordinate system

Figure 1 shows the common definition of the coordinate system for a parabolic collector. The origin is located on the axis of rotation (in general, this does not coincide with the vertex of the parabola) at the front end of the collector, the Z-axis points from the vertex of the parabola to the focal line and the Y-axis in the longitudinal direction. The zenith position (elevation angle = 90°) is reached when the optical axis points vertically upwards. Correspondingly, this axis is parallel to the ground in the horizon position (0° for East, 180° for West)

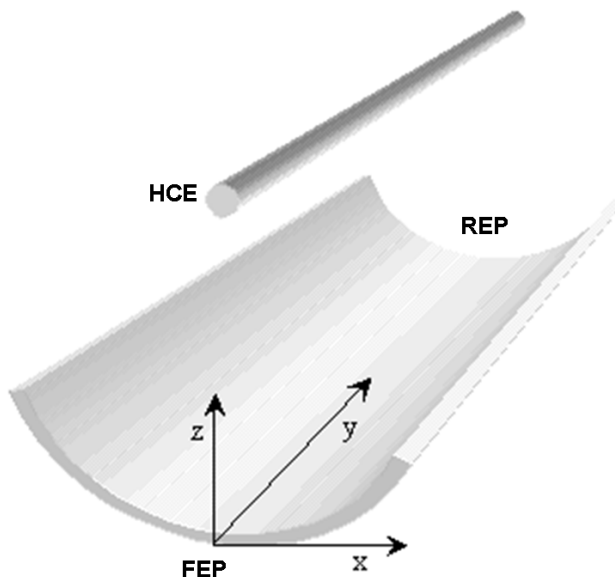


Figure 1: Definition of coordinate axes in the parabolic trough collector



1.3 Measurement quantities

With regards to the solar field's optical performance, all influences by the collector geometry are considered by the Intercept factor (IC). Three independent geometrical properties determining the IC can be distinguished (Bendt, Rabl et al. 1979) (Pottler, Ulmer et al. 2014).

The shape accuracy of CSP concentrators is commonly represented by slope deviations in X-direction (**SDX**) and slope deviations in Y-direction (**SDY**).

In the case of PTCs, tracking deviation (**D_Track**) can be described by the projection of the incidence angle on the focal plane (see: Sec 2.1, Fig. 2.1 in (Bendt, Rabl et al. 1979)

Absorber tube deviations from the focal line are described by **D_Abs_x** (normal to the optical axis and normal to the axis of rotation) and **D_Abs_z** (parallel to the optical axis).

In general, the concentrator geometry is also affected by ambient conditions and load cases.

1.3.1 Mirror shape

For the mirror shape accuracy, either slope- or 3D-shape deviations can be measured and assessed. For the optical performance, the slope is the relevant parameter as the deviation of the reflected ray in the receiver region is determined mainly by the direction of the surface normal vector, while the exact 3D position has a minor effect.

SDX and **SDY** (Lüpfert and Ulmer 2009) are considered to be the fundamental property for any CSP concentrator system (see Figure 3). **SDX** and **SDY** depend on compliance of the individual components (glass mirrors and support structure) with the tolerances, assembly accuracy, and on the interaction or support structure and mirrors for different load.

For point concentrating systems, both **SDX** and **SDY** are of equal importance. For line concentrating systems like the PTC and Linear Fresnel Concentrator (**LFC**), the relevance of **SDY** depends on the angle of incidence ($\phi_{||}$): **SDY** can be neglected for $\phi_{||} = 0$, while for increasing $\phi_{||}$, **SDY** contributes substantially to the reduction of the **IC**. Generally speaking, the impact of **SDX** on the annual energy yield, for line concentrating systems, is ten times higher than the impact of **SDY** (p. 5 in Ulmer, Steffen et al. 2009).

Slope deviations are defined as the difference between ideal and real surface normal vectors, projected onto the XZ or YZ plane:



$$SD_{X,Y} = \arctan \left(\frac{\overrightarrow{N_{X,Y}^{real}}}{\overrightarrow{N_Z^{real}}} \right) - \arctan \left(\frac{\overrightarrow{N_{X,Y}^{ideal}}}{\overrightarrow{N_Z^{ideal}}} \right)$$

A special sign convention (see Figure 2) is used to simplify the interpretation of measured data, by turning the sign so that negative slope deviations denote too steep mirror areas (the reflected ray passes below the design focus) and positive slope deviations denote too flat mirror areas (the reflected ray passes above the design focus). The Focus deviation **FDX** combines the **SDX** with the distance between mirror and receiver. This quantity can be directly compared with the receiver tube diameter.

$$FD_X = SD_X \cdot 2 \cdot |RF|$$

RMS values of both slope- and focus deviations are used as input parameters for statistical Ray-Tracing (RT) as described in (Pottler, Ulmer et al. 2014) . The correct (equal) weighting of single **SDX** values to obtain the **RMS_{SDX}** is achieved by a homogeneous spatial resolution of measurement samples N in the aperture area:

$$RMS_{SDX} = \sqrt{\frac{\sum_1^N SD_X^2}{N}}$$

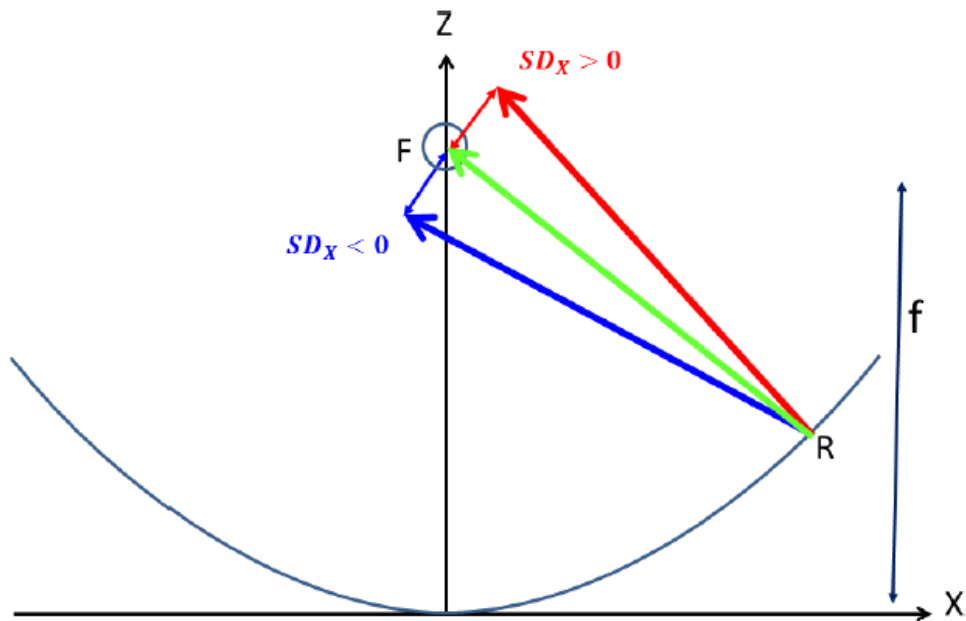


Figure 2: Cross section showing the optimal direction of reflected radiation (green) of the parabolic mirror and the influence of positive (red) and negative (blue) SD_X . For negative X values, this convention remains valid. The distance between point of reflection R and design focus F is used to calculate FDX .

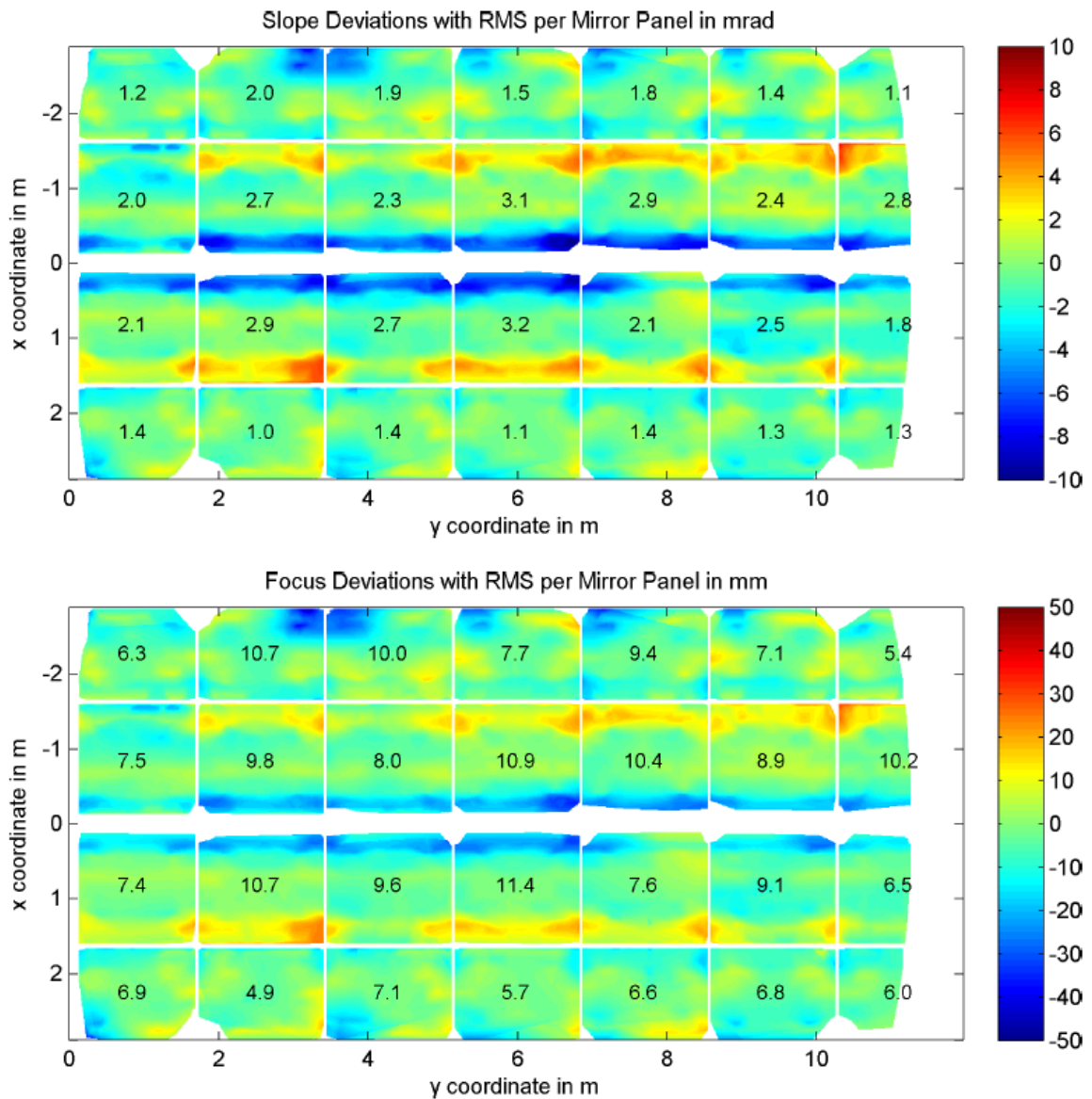


Figure 3: SDX (top) and FDX (bottom) maps for a RP3 SCE at the KONTAS facility at PSA. The numbers denote RMS values per mirror panel. Rather high absolute SDX values close to the parabola vertex (blue in the top figure) are converted into relatively moderate FDX values due to the short distance between mirror and absorber. On the other hand, SDX values at the outer mirror rim result in comparatively high FDX values due to the increased distance to the absorber. The overall performance of this module is excellent with an IC of approx. 99% when neglecting blocking and shading of the HCE bellow protections. The data was acquired with airborne deflectometry.

1.3.2 Receiver position

Typical HCE for \PTC consist of a stainless steel tube with adiameter in the range of 70 - 90



mm. All HCE designed for high temperature applications are surrounded by an evacuated glass envelope tube with an anti-reflective coating to minimize convection heat losses and to maximize the transmittance. A spectral selective coating of the steel tube assures high absorptivity low radiative heat losses. The cost share of the HCE is about 7% of the total investment cost of the entire plant (WorldBank 2010). Thus, HCE can be regarded as a sensitive key component. In order to harness the full performance, the deviation of the tube centre line from the focal line (**D_Abs_x** and **D_Abs_z**) must not exceed the specified tolerances. These tolerances are mainly determined by the aperture width of the PTC and the absorber tube diameter. For the RP3 mirror geometry and quality, deviations up to 5 mm are tolerable without significant performance loss. NREL (Owkes 2012) highlights the necessity to measure deviations of the receiver tube from the focal line, as their impact on the optical efficiency is in the same order as slope deviations of the mirror surface.

1.3.3 Tracking deviation

PTCs as one axis tracking collectors require precise and reliable adaption of tracking angle under all operating conditions, according to location, time of the year and tracking axis orientation.

D_Track occurs if the absolute angle between the optical axis of the concentrator and the sun position, projected on the YZ (focal) plane of the concentrator is greater than zero.

It can be caused by malfunction of the tracking system (mechanics, sun position algorithm, and optional sun-sensors), or misalignment of adjacent SCEs during solar field assembly.

The local direction of the optical axis along the SCA may also be altered by operational loads like wind, static unbalance and bearing friction.



2 Measurement methods

An overview on state of the art measurement techniques to obtain the geometric accuracy of collectors including effects operational loads on the structure and tracking errors is presented in the following. Further reviews and comparisons on this topic can be found in (Xiao, Wei et al. 2012)

2.1 Scanning methods

Scanning a reflective surface with a well-defined light source and observing the direction of the reflected ray is the most intuitive and directly arising approach. The measurement uncertainty is related to the accuracy of the position of light-source, point of reflection, and detected hit point of the reflected ray usually on a diffusely reflecting surface. Among the available methods for scanning CSP collector slope measurements, VSHOT is the most advanced laser ray-trace system, which can be applied to both point- and line-focusing CSP concentrators (Wendelin, May et al. 2006; Lewandowski and Gray 2010)

2.2 Deflectometry

Deflectometry or fringe reflection uses known regular stripe patterns on a screen or target whose reflection in a specular surface is observed by a digital camera (Knauer, Kaminski et al. 2004). From the deformation and distortion of the stripe pattern in the reflection, the local normal vectors of the mirror can be calculated. This method is applied to measure the geometry of heliostats of solar power tower (SPT) plants (Ulmer, März et al. 2011), parabolic Dish Collectors (PDC) (Ulmer, Heller et al. 2008), Linear Fresnel Reflector (LFR) mirror panels (Heimsath, Platzer et al. 2008) or single mirror panels of PTCs {März, 2011 #84} and has reached the maturity of a commercial system for in-line mirror production quality assurance (Weber, Ulmer et al. 2014). The application of this method to a full-size PTC module in production environment has been also successfully implemented (Ulmer, Weber et al. 2012). However, the need for large screens and disturbance by ambient light complicates the implementation deflectometry as a field measurement tool. In order to overcome these



restrictions, there are several methods that use the absorber tube as a “pattern” to determine **SDX** or at least rough performance measures. These methods are based on the Distant Observer (DO) method proposed by (Wood 1981)

- TOP involves overlaying theoretical images of the absorber tube in the mirrors onto surveyed photographic pictures (Diver and Moss 2007) and iterative improvement of the mirror alignment. It uses an array of several ground based cameras to align mirror panels of horizontally orientated PTC modules.
- Another ground based tool for the optical alignment of parabolic troughs called VISfield was developed by ENEA (Montecchi, Benedetti et al. 2010). After manual alignment of the HCE, the local mirror slope and IC values are derived from digital images, and positions of camera, absorber tube, and absorber tube-edge reflections.
- TARMES (Trough Absorber Reflex MEasurement System) was developed to achieve high accuracy and high spatial resolution and produces SDX maps from a set of photos (Heinz 2005; Ulmer, Heinz et al. 2006; Ulmer, Heinz et al. 2009). Normal vectors of the mirror surface are derived from the spatial coordinates of the absorber tube edges, the position of the absorber tube edge reflex on the mirror surface and the nodal point of the camera. The measurement principle of TARMES is presented in REF_Ref482280782 \hFigure 4.
- NREL (Owkes 2012; Stynes and Ihas 2012) has developed an optical measurement tool using the centre line of the image of the reflection of the absorber for PTC that measures the combined errors due to absorber misalignment and reflector slope error similar to TOP and TARMES. By measuring the combined reflector-absorber errors, the uncertainty in the absorber location measurement is eliminated. As the IC depends on the combined effects of the absorber alignment and reflector slope errors, it is stated, that the combined effect provides a simpler measurement and a more accurate input to the IC estimate. This method has also been considered for airborne data-acquisition.

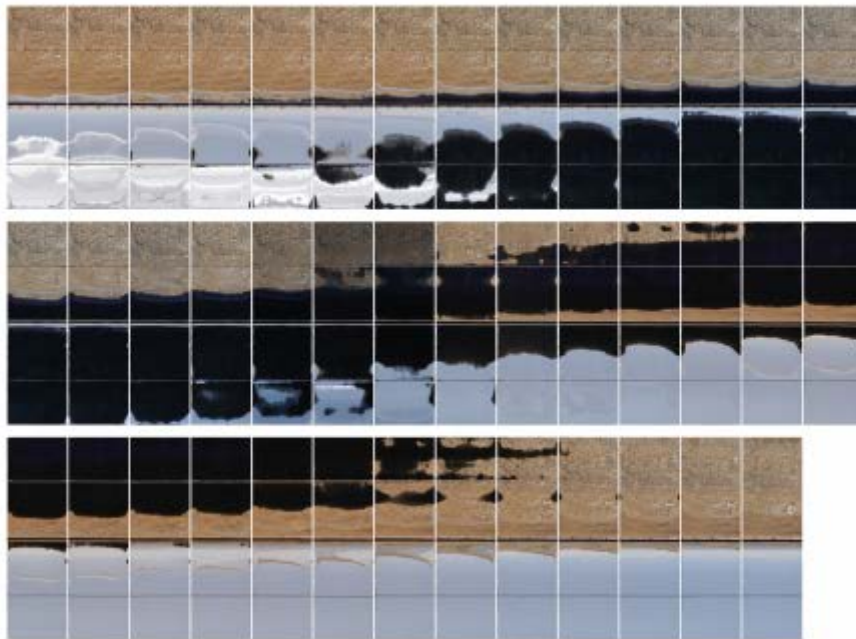
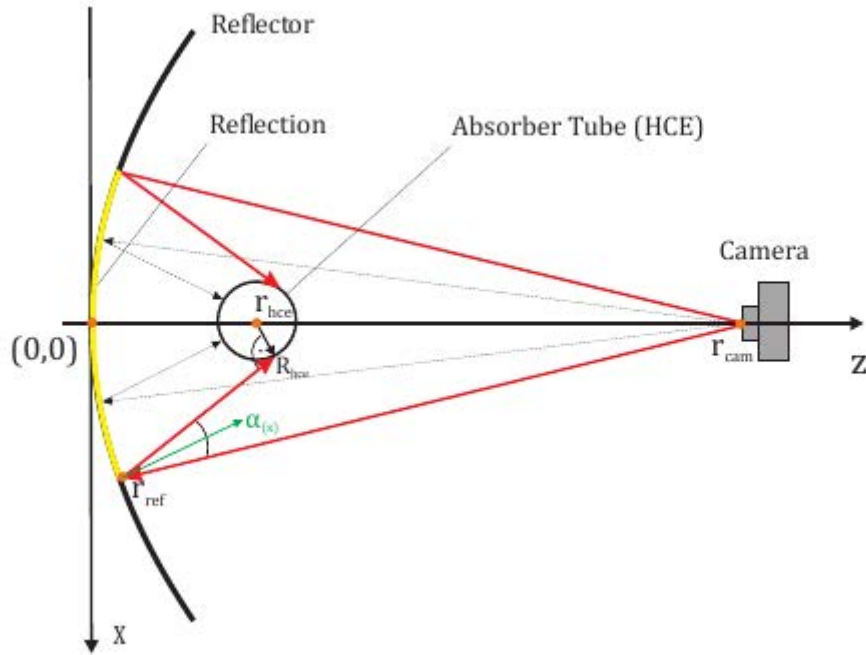


Figure 4: Top: Cross section showing the relevant measurement points of the TARMES approach. The reflection of the absorber tube edge in the mirror surface is observed by the camera. The bisecting line of an angle delivers the local slope along the edge reflection. Bottom: Image series of a single mirror row from a TARMES measurement with the SCE facing horizon the upper half of the collector shows reflections from the ground, while the lower part reflects the sky. At least 40-60 images are required to achieve sufficient covering of absorber tube edge reflections over the entire mirror surface.

Most previously mentioned methods (VSHOT, VISfield, TOP, and TARMES) have in common that the collectors are easily measured facing horizon, while the measurement of a



collector module in its prevailing operating position (around zenith) involves considerably increased effort. The typical scope of one measurement is a single SCE, so these methods are suitable for random sampling. So these methods are not suitable for entire solar field characterization.

2.3 Photogrammetry

Close range photogrammetry (PG) (Luhmann, Robson et al. 2006) has been applied to various CSP collectors (Shortis and Johnston 1997; Pottler, Lüpfer et al. 2004). This technique derives the coordinates of points of interest, highlighted by special markers from a set of images taken from different positions. The application of these markers to large collector surfaces or structures means a high preparation effort. Photogrammetry can be applied to any collector orientation and with sufficient spatial resolution to detect characteristic shape deviations of mirrors and other points of interest like absorber tubes or axes of rotation. It is especially suitable for deformation analyses of prototypes and in cases where no reflective mirror surfaces are mounted. As the spatial resolution depends on the density of markers, it generally delivers a lower resolution than deflectometric approaches. Post-processing of the raw images is a two stage process. The first step is the calculation of properly scaled but arbitrarily orientated 3D coordinates from raw images using commercial image processing and bundle adjustment software. The following task of calculating CSP specific deviations and performance issues in general is carried out by custom software. The calculation of shape, slope and absorber tube deviations consists in comparing measured and design coordinates.

2.4 Others (not part of the protocol)

Recent developments in commercial laser scanners/radars allow their use to measure 3D coordinates of larger surfaces as parabolic trough modules or heliostats. Specular reflecting surfaces need to be coated with an opaque paint before performing the measurement. A Laser radar has been used (Ulmer, Weber et al. 2012) to validate a deflectometric measurement on an entire parabolic trough module.

Coordinate metrology using a coordinate measuring machine (CMM) has been applied to single mirror panels as validation against other approaches (King, Comley et al. 2014)



3 Protocol for characterization of complete solar concentrators with photogrammetry

This measuring protocol deals with the photogrammetric shape measurement of linear concentrators for solar thermal power plants, in particular Parabolic Trough Collectors (PTCs). The compliance with the tolerances, which are unusually small for components and structures of this dimension in constructional steelwork, is of great importance for the optical efficiency of the collector.

Due to its accuracy and flexibility, photogrammetry has proven itself as a measuring method for both prototypes as well as on-line quality assurance in production. There are fundamental differences between measurements on reflective surfaces and bare collector structures only. Photogrammetry is mainly used for the measurement of the structure, whereas the deflectometry (TARMES) is more advantageous in the case complete collectors with mounted mirror panels because of its high spatial resolution. Close range Photogrammetry allows measuring the position of the mirror surface in relative to the focal line and to the axis of rotation. Furthermore, there is the possibility of precise and high-resolution deformation analysis between different tracking positions and under operational loads.

Before starting a measurement campaign, the geometry of the collector should be known order to prepare measurement adapters and to provide a sufficient number of suitable targets. If possible, technical drawings should be requested. With this information, the measurement campaign can be prepared, in particular the number and application of the targets and measurement adapters. A certain infrastructure is also required. This involves mainly a mobile man-lift and sufficient space to move around the collector.

On site, the collector is equipped with the target marks, which is, according to experience, the most time-consuming part of the measurement.

The basic principles of acquisition of the images for the photogrammetric measurement images and the photogrammetric evaluation are presumed to be known and hence, they are only briefly treated.

The evaluation is divided into two parts:

- The 3D coordinates are determined from the measurement images in the



photogrammetric part of the evaluation. For this purpose, commercial software, e.g. the Aicon 3D Studio, Photomodeler or VMS can be used.

- In the second part, the parameters relevant for the optical properties of the collector are determined from the obtained 3D coordinates. Before doing this, we recommend an accuracy analysis and scaling.

3.1 Points of interest

Measurement locations (also called Points of Interest – POI .) of a PG measurement must be highlighted with circular markers. For outdoor measurements, it is in most cases necessary to use retroreflective markers (Reflexite VC 200-5) in combination with a (ring-) flash, to obtain sufficient contrast between markers surface and background. However, it is also possible to fully cover mirror surface with a printed plastic film.

The selection and preparation of the POIs is described in the following. Depending on measurement volume and spatial resolution, this preparation consumes about up to 80% of the total time required for the measurement, while the image acquisition is less costly. For this reason, the accurate and careful preparation is mandatory for meaningful results.

3.1.1 Points to be measured on PTC steel structures

Figure 5 gives an overview of the steel-structure of an SCE whose design corresponds to the EURO-Trough geometry. The stability is mainly achieved by the torque box design. The HCE supports are fixed on the top of the torque box. There are 14 cantilevers on each side of the box to support the mirror panels. At the ends of the torque box, there are front- and rear end plates, which support the rotating axis and constitute the connection to the next SCE.

Parabolic trough collectors of other types may deviate considerably from this design. Thus, instead of the torque box, a tube with a corresponding diameter can be installed; the number of cantilevers and the mirror supports may vary. Collectors made of materials other than steel (e.g. sandwich or composite structures, metal sheet mirrors) have, in general, a totally different geometry. However, the coordinates to be determined and described in the following are still valid.

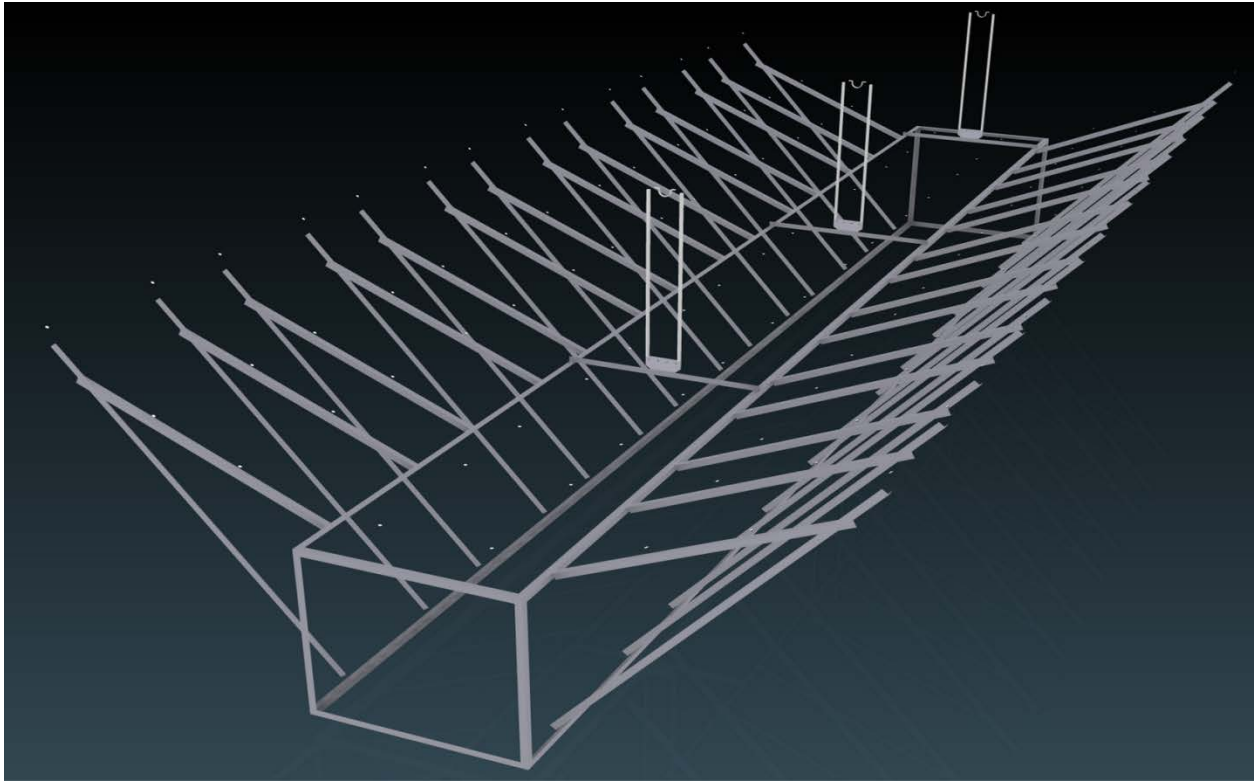


Figure 5: 3D sketch of the steel structure of a collector in torque box design.

3.1.1.1 Absorber tube

The position of the absorber tube (HCE) must be determined in particular in the X- and Z-direction relative to the mirror surface. The centre of the HCE should coincide with the focal line within ± 5 mm for the RP3 geometry. Due to the different thermal expansion of structure ($\Delta T = 50$ ° K) and absorber ($\Delta T = 450$ ° K), the HCE supports allow for thermal expansion the Y-direction. This results in the following relevant measuring points:

- If no absorber tube is installed, a special HCE support adapter is used, which allow to measure the position of the centre of the support and thus the expected position of the mounted HCE.
- If no absorber tube is installed, the HCE supports are tilted in the Y-direction, so that a direct comparison of the measured- and design-data is not possible. It is also mandatory to measure the supports axis of rotation. That way that the coordinates can be corrected by virtually lifting the supports to vertical position.
- When the absorber tube is installed, its centre of the steel- or glass-envelope tube and thus possible deviations from the focal line can be determined directly. For this



purpose, at least three targets are placed concentrically on the pipe. From these points, the centre of the absorber can be determined by circle fitting algorithms.

3.1.1.2 Collector longitudinal axis

The determination of the Y-axis is in particular important for the transformation of the arbitrarily orientated raw data into the design coordinate system. Depending on the accessibility of the rotation axis, this can be achieved in two ways:

- If the rotation axis is easily accessible, these points are suitable for determining the Y axis.
- In all other cases, the vertex of the parabola is more suitable to represent the Y-axis. Due to the dead load of the collector, the vertex is in general curved so that only the vertex points at the Front end plate (FEP) and the Rear end plate (REP) can be considered as relevant for the Y axis determination.

The discussed transformation is discussed in more detail in Section 3.8.2.

3.1.1.3 Water-level

In some collectors, there are two bore-holes in the FEP and REP, which define the X-axis. These reference points are used to align the SCEs in the field. The connection line of these bores can be measured with an appropriate adapter. In the evaluation, these points can also be used for the virtual alignment of the module.

3.1.1.4 Mirror mounting points

For state of the art parabolic troughs based on a steel structure and glass-mirrors, each mirror panel is attached to the metal structure by means of 4-6 tilted metal clamps to determine the centre of the round or long hole in the clip, target marks are centered with a suitable adapter in the bore-hole.



3.1.2 Changes in the points to be measured with the reflective collector

In the case of the fully assembled collector or in case of a self-supporting construction, which does not rely on a steel structure with glass mirrors (e.g. sandwich structures); the previously described procedure has to be adapted.

This requires, on the one hand, the use of other materials of the target-marker (PVC film, stickers); on the other hand, the positioning of the targets and the evaluation must also be changed.

In order to determine the structure of the (steel) structure supporting the mirror panels, the positioning of the targets on the mirror top should be realized in such a way that they are located directly above the fixing points. This can be achieved by the use of templates. Additional targets on the mirror surface are used to determine deviations from the desired shape and deformations between different operating positions with a higher spatial resolution. Approx. 40-100 target marks per square meter of mirror area should be installed to reproduce characteristic deformation pattern.

If the axis of rotation is not accessible, the parabola vertex should be defined as Y-axis.

An important part of the evaluation is the determination of the parameters for the transformation of the measured data into the design data coordinate system. As described in section 3.8.2, it is also necessary to determine a rotation angle about the Y-axis. The angles between pairs of corresponding mirror-mounting points can be used directly for this purpose.

3.2 Measured quantities and results

After the raw 3D point cloud has been scaled and transformed into the target coordinate system of the design data, the deviations between the measured points and the design data can be determined directly in each dimension. However, to assess the optical performance of the collector, these simple difference-values are only suitable to a limited extent. Rather, the information of different points must be linked to each other, taking into account the collector geometry. The following section describes these performance variables in more detail.

3.2.1 SDX (depending on spatial resolution)

Coarse slope deviations in curvature direction (SDX) can be determined for only the pairs of mirror mounting points. This provides a general estimate for the overall orientation of the mirror panel. An important parameter in this context is the angle between mirror mounting points belonging to the same facet and mounted on the same cantilever (see Figure 6). The orientation of the facet is determined by the angles alpha and beta, so that their values affect significantly the optical performance.

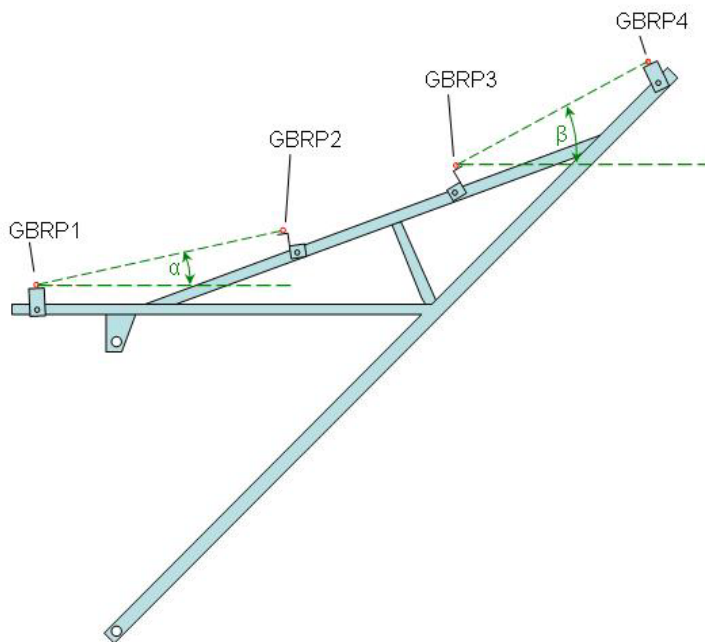


Figure 6: Cantilever of RP3 collector with definition of alpha- and beta angles

The optical quality of a collector with a steel structure is determined by the shape of the individual mirror facet as well as by the geometry of the steel structure. By using additional markers between the mirror mounting points, also the individual shape of the mirror panel itself can be deduced. Here, the spatial resolution depends on the density of markers and in general, a lower resolution compared to deflectometric methods is achieved.

3.2.2 Local angles of the mirror mounting points

Mirror panels consist in general of relatively thin glass (4-5 mm) so their shape is highly sensitive to any load. These loads can be distinguished in external and internal loads.



External comprise e.g. wind and dead load. Internal loads are caused by tension and stresses caused, if the shape of the mirror panel does not perfectly match the structure. This can be caused by incorrect positions of either the mirror panel mounting pads and/or the collector structure. An important parameter in this context is the angle gamma of the mirror mounting bracket surface relative to the X-axis (see Figure 7).

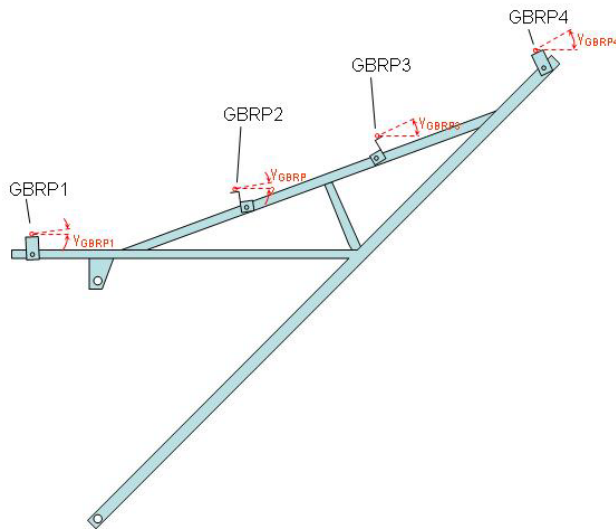


Figure 7: Cantilever with definition of gamma angles

Gamma should correspond to the tangent of the parabola at this point. Deviations cause local stress and a large-scale deformation of the mirror panel. For the random sampling of the gamma angle, some GBRPs can be equipped with measuring adapters. It must be ensured that the brackets are not deflected by the weight or the unbalanced measuring adapter! Alternatively, said angles can also be determined with an inclinometer.

3.2.3 Deflection by dead load in zenith position

For the comparison of the mirror shape and of the absorber tube position with the reference data, the deflection of the module due to dead load must be corrected. For a single, standalone SCE, a parabolic function is suitable to describe the deflection of structure and absorber tube:

$$dz = dz(y, y^2)$$

The associated parameters can be determined from the Y and Z values of the innermost row of mirror attachment points or directly from the vertex points. SCEs connected to the drive pylon or to neighbouring SCEs show a distinct deflection curve, which depends on the



mechanics of interconnection and the collector structure.

3.2.4 Deformation between different operating positions

For the optical performance, the shape of the collector in the zenith position is primarily relevant. The collector shape may also be measured for other elevation angles. On the one hand, the performance of the collector can be assessed for these positions. On the other hand, the relative deviation of the module can be investigated. This involves sagging of the absorber tube and mirror panels and twist/torsion due to static unbalance. For the comparison of the geometry in different operating positions, the resulting 3D point clouds must be matched. For the determination of these transformation parameters, there must be at least three points which:

- do not significantly change their position during the rotation
- are not collinear
- are ideally distributed over the entire collector.

This condition is most likely met by the axis points to FEP and REP as well as an HCE near one of the endplates. Via these points, the measurements belonging to different operating positions can be matched via a system adaptation. For all other points present in both measurements, the deformations into the respective spatial directions can then be calculated. The Z- and X-directions are most important in this respect.

Provided that the collector is balanced, the following phenomena are primarily observed:

- Similar to the deflection in the negative Z direction in the zenith position, a deflection occurs at other angles of rotation, but the centre of the structure is then increasingly displaced in the X-direction.
- The line² at which the second moment of area acts against the torsion does in general not coincide with the principal axis of inertia. For this reason, a torsion increasing towards the collector centre is observed. This twist/torsion is equivalent to



a tracking error. In the case of rigid structures, this effect is visible in the data but is not relevant to the performance. However, for modules with comparatively low torsional stiffness, the respective position of the absorber tube should be compared with the focal line and the torsion.

3.3 Tolerances

The definition of tolerances for measures accessible with close range photogrammetry involves the careful balancing of all involved variables. The tolerances can be either set by defining a design Intercept factor (normally around 97 to 99%) and then by iteratively investigating the sensitivity of the IC on geometric deviations by numerical or statistical raytracing. The latter is based on the concept described in (Bendt, Rabl et al. 1979) and involves the creation of an “effective source” by combining the sunshape with the RMS value of geometrical imperfections. This determination of the tolerance values and the whole process takes place in close collaboration with the collector manufacturer. Therefore, at this point, only a list of the parameters relevant for the tolerances is provided:

- Focal length
- Absorber tube diameter
- Aperture width
- Target intercept factor
- Sunshape
- Expected tracking error (drive, control, misalignment and torsion)
- Mirror shape of installed glass mirror panels
- Expected deviation of the absorber from the focal line

The total error of the collector is given by the four last-mentioned values, while the sunshape is included as a fixed quantity, mainly depending on the average conditions of the atmosphere. The rule of the thumb is that the shorter the focal length and the larger the HCE diameter, the higher is the intercept factor for a given total effective beam spread. Or in other words, systems with a lower concentration factor tend to be less susceptible to geometric inaccuracies.



3.4 Equipment

A tabular listing of the equipment is given in Table 1.

First of all, a high-quality digital mirror reflex camera (e.g.: Nikon D2, D300, Canon EOS 5D, Canon EOS 1D) is required for a photogrammetric measurement. Such models are characterized by high mechanical stability and image quality. As measuring marks, so-called Hubbs targets³ or similar models⁴ have proven themselves for the localization of boreholes. For surfaces and mirrored modules, self-adhesive or magnetic foil targets can be used. Depending on the evaluation software used, so-called coded targets play an important role. These provide an interrupted, concentric ring around the actual measuring dot, with which the number of the point is encoded. The use of coded target marks and the corresponding software leads to a considerable time-saving in the evaluation. The properties of the target-markers depend on the ambient light. For outdoor measurements, retro-reflective targets and the use of a ring flash are recommended. A proven retro-reflective film for this application is Reflexite VC 200-5.

Reference bars provide some targets with accurately known distances, which can be used for calibration and assessment of the measurement accuracy.

Item	Description	Example
High-quality digital SLR camera	Resolution > 12 Mega pixel	Nikon D2, D300 Canon EOS 5D, 1D
Fixed lens	Fixed focal length (no zoom lens!)	Nikon 20mm f/2.
Ring flash	Symmetric flash illumination with respect to the optical	Sunpak auto16R pro

3

<http://hubbsmachine.com/4-retro-reflective-contrast-photogrammetry-targets>

4

<http://www.cspservices.de/products-services/catalog/categories>



Item	Description	Example
	axis of the camera assures homogenous visibility of the targets	
Batteries	For flash do not use rechargeable batteries, as they do not provide the required performance at lower temperatures	
Retroreflective target marks, as stickers, on PVC foil	Circular target stickers. A ring of black foil around the retroreflective area greatly enhances contrast and such detection rate on bright surfaces	Reflexite VC 200-5
Retroreflective target marks, with adapters for boreholes to be measured and long holes.	Special retro-reflective targets with a pin used to detect the position of drillings/holes	Hubbs of PG targets
Articulating Boom Lift (aka: Cherry Picker ⁵)	For preparation and image acquisition.	
Calibration bars/-rods for determining the measuring accuracy		
Reference system		
Protective equipment for working at height		

5

https://en.wikipedia.org/wiki/Cherry_picker



Item	Description	Example
Cable ties, small items		
Software for PG and post-processing		

Table 1: Equipment for the photogrammetric measurement of parabolic trough collectors

3.5 Boundary conditions

The boundary conditions have an important impact on the results of the photogrammetric measurement.

Parameter	range	comments
Ambient light		
Wind	< 4 m/s	
Precipitation	No rain during preparation and measurement. Water droplets will alter the appearance of the targets	
Space requirements	> 4 m around collector outline	
Collector status: Cleanliness	Cleanliness > 0.99.	
Collector status: HTF temperature	Constant (+/- 10°K)	
Collector status: Elevation angle	90° or depending on measurement objective	

Table 2: boundary conditions for the photogrammetric measurement of parabolic trough collectors

3.6 Preparations



3.6.1 General requirements

The collector to be measured must be supported free of forces. This is necessary to avoid unintentional deformation resulting from the interaction of structure and supports. This prerequisite is fulfilled, if the SCE is supported by two pylons and freely rotatable, or the torque box on the ground is supported at three points (no over-determination of the supporting system). Around the collector, there should be enough space to be comfortably operating the man-lift. The reference rods/-bars are distributed uniformly over the collector in the direction of the relevant measuring accuracy (X- and Z-direction). Here, a positioning at the edge of the measuring volume being preferred, as this provides an upper limit of the measurement uncertainty.

After the collector has been completely equipped with the targets, test images should be made from some representative shooting positions (distance and angle of view on the target marks) in order to adjust the parameters:

- flash power
- exposure time
- focus
- ISO sensitivity

Table 3 provides an overview on the recommended camera settings:

Camera parameter	range	comments
ISO	200	
Aperture	Closed (highest value e.g. 22)	
Flash	Adapt flash settings to target reflectivity and distance to obtain a target brightness of 100-200	
Focus	Set to ∞	
Autofocus	off	

Table 3: Camera Settings for photogrammetry data acquisition



The goal is to obtain images with a brightness values between 100 and 200 (with an 8-bit camera), thereby suppressing the effect of the ambient light. If the camera settings are fixed, the aperture and focus adjustment ring should be fixed with adhesive tape.

The camera and the measuring object must not change their geometry during the measurement. If coded target marks are used, a sufficient number of these codes must be distributed over the measured object. The coded marks should not be associated with reference points to be measured (POIs), but merely serve to pre-orient the images. A reference system (consisting of at least five coded targets) is fixed in the centre of the measuring volume. The 3D coordinates of this reference system are known and serves only for the initial orientation of all images.

3.6.2 Placement of markers on structures

At the Points of interest (Section 3.1), (retro-reflective) target-markers are to be placed directly or by using corresponding adapters. The POIs includes:

- Mirror surface
- Mirror attachment points (only collector structure)
- Rotation axis and/or vertex of the parabola
- Absorber tube- and support
- Water-level (optional)
- Angle measuring adapter for gamma angle (optional, only collector structure)
- Possibly further coded auxiliary markers to link badly visible areas with the rest of the measurement volume

If the markers are applied on a curved surface, the maximum allowed diameter of the marker depends on the curvature of the surface. In case of strongly curved surfaces like axis of rotation or absorber tubes

3.7 Data acquisition

The actual photogrammetric measurement consists only of the recording of the measurement images. During this time, neither the measured object (for example, by wind)

may deform, nor should the camera setting change.

The size of a typical PTC in combination with distance restrictions due to the height of the man-lift and the minimum spatial resolution of the markers make it impossible to capture the whole object within a single image. Rather, only individual fractions of the collector are visible, so that images with sufficient overlapping between neighbouring collector sections are required. An overview of possible perspectives for a photogrammetric survey of a collector is shown in Figure 8 **Error! Reference source not found.**

In general, it is advisable to start the acquisition of the first images from the reference cross in order to assure a well-performing pre-orientation. After successful photogrammetric evaluation, the measuring accuracy and the presence of all relevant target marks are checked. If the average measurement accuracy is above the permissible value (this is dependent on the object size and the accuracy required) or if important reference points (for example the axis or vertex points) are missing, further pictures are necessary or the evaluation settings have to be adapted.

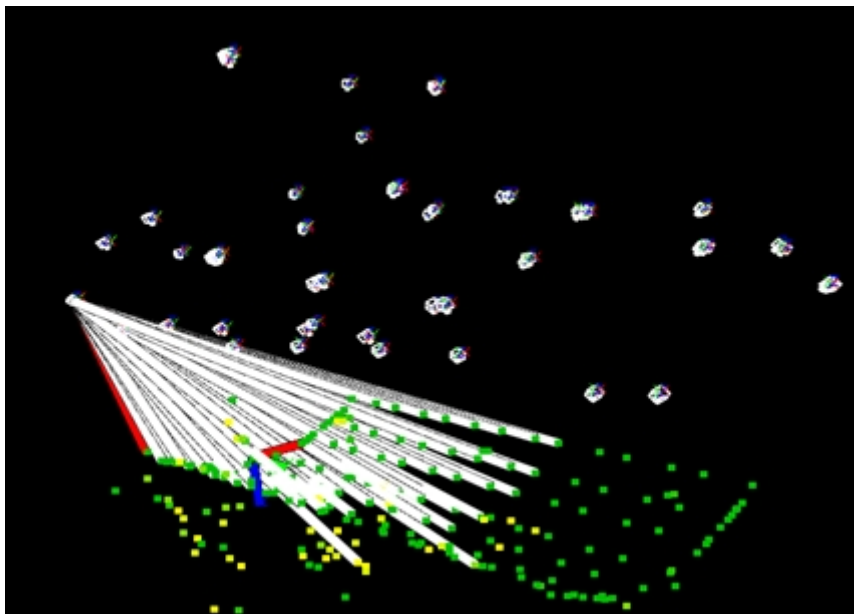


Figure 8: 3D view of a PG setup. Object points (green / yellow), camera location (white), and landmarks (white beams) detected by the camera.



3.8 Evaluation and post-processing

This section deals with the photogrammetric evaluation of the measurement images and the transformation of the resulting 3D point cloud into the coordinate system of the design data. The comparison and assessment of the data is described. The deformation analysis and the presentation and interpretation of the results are briefly presented.

3.8.1 From images to 3D coordinates

In the first part of the evaluation, the image coordinates of the target marks are determined from the images using commercial photogrammetric (bundle-adjustment) software. This evaluation requires as input the reference system, and starting values for the inner orientation of the camera. The number of parameters to be customized in this part of the evaluation is limited and, under good measuring conditions, little input from users is required when using high end software. For the accuracy analysis it is recommended to use the calibrated distances between the target marks on the reference bars (if deployed). On the basis of this data, the point cloud is scaled and the measurement accuracy is estimated on the basis of the remaining deviations. If the reference bars have been placed on the edge of the measuring volume, the derived uncertainty can be assumed to be an upper limit for the rest of the POIs.

The 3D coordinates are then available for further evaluation. Each 3D point is identified by its number (# ID). Since un-coded target marks are randomly numbered by the photogrammetry software, the points have to be renamed according to the nomenclature of the evaluation.

If adapters were used to measure invisible or poorly accessible points, the corresponding adapter correction is now performed to determine the target POI.

3.8.2 Transformation of measured data into the design data coordinate system

In principle, there are several possibilities to transform the measured data into the coordinate system of the design data. A best-fit with minimization of the quadratic deviations taking all coordinates into consideration is at first glance the most straight-forward and intuitive solution. However, there is a risk that performance parameters derived that way will not adequately represent the collector's optical performance. In the case of flat or mirrored



modules, there is also the problem that there is no reference data available for the measured points on the (mirror-) surface. In this case, an attempt was made to project the measured points onto a parameterized surface, and iterative to minimize the deviations. This method, among other things, has also proved to be unsuited for this application because of the high computational effort involved.

An alternative solution to determine the transformation parameters emphasizes the role of the axis of rotation and the focal line. This method has the advantage, that the resulting performance parameters are derived under consideration of realistic boundary conditions concerning mutual orientation of mirror, tracking axis and absorber.

In the following, M is the set of measured 3D points, T is a linear transformation, and R represents a rotation matrix. Assuming that the points on the module's longitudinal axis (represented either by the parabola vertex or by the rotational axis at FEP and REP) have been determined with sufficient accuracy, the following procedure should preferably be used:

1. The FEP is transformed into the origin ($M1 = M + T$)
2. The REP is transformed to the Y axis by

- a. $M2 = M1 * Rx$

and

- b. $M3 = M2 * Rz$

using two successive rotations around the X and Z axes, so that

$$X_{REP} = Z_{REP} = 0$$

Now the only freedom degree is the rotation around the Y axis. The corresponding angle of rotation can e.g. been determined via the deviations of the alpha and beta angles (see Figure 6) from the design data.

3.8.3 Additional correction measures

Depending on the state of the module, further corrections must be made before the comparison with the design-data can be done. If no absorber pipe is mounted, the tilted HCE supports are virtually positioned perpendicular to their measured axis of rotation. In some collector models, the cantilevers may also be twisted about an axis parallel to the Z axis. After these effects have been corrected, the rotations described in the previous section 3.8.2



must be repeated!

3.8.4 Comparison with nominal data and determination of the collector quality

After the transformations of the measured data onto the design data and the corrections have been performed successfully, the deviations of the mirror points and of the absorber tube are obtained directly from the difference between the two data sets. Angle deviations are determined from the difference between the X and Z values of the corresponding mirror mounting points. The distances relevant for the mirror mounting are calculated from the connection vectors of the mirror mounting points belonging to a single mirror panel. The individual deviations may be used to calculate statistical values and for the comparison with the tolerances, so that an objective assessment of the collector quality is possible.

3.8.4.1 Aspects for the complete module with attached mirror panels

If the structure is to be assessed for the mirrored collector, the calculated alpha / beta angles cannot be directly compared with the desired data due to the uncertainties when attaching the target marks. Rather, the design values must be calculated at the X-positions using the focal length and the glass thickness. Based on the design position at the specific X locations, the design angle values for alpha and beta are obtained. This also applies to collectors with a flat, self-supporting substructure.

3.8.5 Deformation analysis

To show the deformation between different operating positions (elevation angles), the reference dataset (zenith = 90°) should already be aligned as described in section 3.8.2. The 3D point clouds obtained from measurements in other elevation angles or load cases are transformed onto the reference case by a best fit of at least three targets that are expected to show least deformation. The deformation analysis is carried out by analysing the difference of the remaining identical points.



3.9 Data format

Due to the variety of photogrammetric- post processing software, a meaningful definition for the data format for the data exchange is presented below. The file-type should be an ASCII text file, containing the IDs, coordinates and further information of each POI. The decimal operator is the dot (.).

The elementary version of the file contains only four columns, whereby the first column denotes the POI ID and the remaining three rows provide the position in XYZ coordinates. The structure of files containing additional information is described below:

File Structure:

1. Column POI ID
2. Column Object coordinate X
3. Column Object coordinate Y
4. Column Object coordinate Z
5. Column Standard deviation in X
6. Column Standard deviation in Y
7. Column Standard deviation in Z
8. Column Deviation or deformation in X
9. Column Deviation or deformation in Y
10. Column Deviation or deformation in Z

In addition, the file header or filename should contain unequivocal information on the way the data was obtained and treated.



4 Protocol for characterization of complete solar concentrators with the distant observer method

As presented in Section 2.2, there are various implementation of the Distant Observer (DO) method proposed by (Wood 1981). Based on the example of the TARMES method, the general requirements and steps for preparation, data acquisition, and evaluation are presented here. Certainly the requirements for other implementations like TOP, VIS-Field, etc. may vary to certain degree, but the scope of the protocol and the lack of details from other implementation allow only the presentation of a single version of the DO deflectometric parabolic trough characterization.

This document gives a step-by-step instruction for a manual TARMES measurement (Heinz 2005; Ulmer, Pottler et al. 2007; Ulmer, Heinz et al. 2009) of a single parabolic trough module. From the reflex of a well-known object (receiver tube), the slope deviation of a parabolic trough is calculated. To get the slope deviation along the X-axis, the collector is turned in a certain angle range while a camera in a relatively large distance (> 30 m) takes the measurement photos. It comprises the following steps:

- installation of the inclinometer(s)
- positioning of the camera
- setup of the measurement devices
- configuration of the measurement
- and measurement procedure, consisting of
 - image acquisition
 - inclinometer reading
 - camera position measurement relative to the parabola vertex

The evaluation is described in Section 4.5.



4.1 Equipment

The equipment for the TARMES measurement serves to capture images and to determine the camera position relative to the concentrator. The equipment is adapted for field measurements and consists only out of off-the-shelf components.

Item	Description	Example
Digital SLR camera	Resolution > 12 Mega pixel	Nikon D300 camera or similar
Camera auxiliary equipment	remote release	ML-L3 Wireless Remote Control
Tripod		
Inclinometers	High accuracy inclinometers	WYLER ZEROTRONIC C
Inclinometers auxiliary equipment	Cables and communication hardware, connection to data acquisition PC	WYLER
Notebook		
Laser distance meter		LEICA DISTO A8
Articulating Boom Lift (aka: Cherry Picker ⁶)	Working height ~35 m	
Further auxiliary equipment.		

4.2 Boundary conditions

The boundary conditions and constraints for the TARMES or any DO measurement are more restrictive compared to Close Range Photogrammetry. The image quality is much more affected by ambient light and the optical properties of the involved components (mirror and

6

https://en.wikipedia.org/wiki/Cherry_picker



absorber).

Parameter	Range	comments
Ambient light	Daylight, ideally cloudy sky. In case of high DNI, the relative position of sun, SCE, and camera must be considered in order to avoid reflections from the sun	
Wind	< 4 m/s	Higher wind values especially in zenith measurements lead to shaking of the man lift
Precipitation	No rain during preparation and measurement. Water droplets will alter the appearance of mirror surface	
space requirements	> 17 m for horizon measurements	See Section 4.4.2
Collector status: Cleanliness	Cleanliness > 0.99.	
Collector status: HTF temperature	Constant (+/- 10°K)	
Collector status: Elevation angle	90° +/- 10° for zenith measurements 0° +/- 10° for horizon measurements	



4.3 Preparations

4.3.1 SCE module

There has to be an operative control unit for the drive, an operator and a power supply (power generator) available on site to turn the collector.

White plastic protection sleeve of the receiver tubes have to be removed one day before the measurement starts.

The mirror panels and the receiver have to be cleaned properly one day before the measurement starts.

The mirrors have to be dry (be aware of dew in the morning).

4.3.2 Equipment

4.3.2.1 Man lift

For zenith measurements, a man lift with a height of at least 35 m (115 feet) has to be available on site. It should be possible to reach the module from both sides.

4.3.2.2 Inclinometer mounting

The following description refers to the use of WYLER Zerotronic inclinometers. When different devices are used, please refer to the corresponding user manual.

Inclinometer mounting and data readout:

- The blue type (Wyler) label has always to face upwards, because the inclinometer is calibrated in this orientation.
- The inclinometer has the highest accuracy in horizon measurement angles. Thus, install the inclinometer horizontally after the collector was turned to the initial collector angle. Thus, install it in an angle where it is expected to be al-most horizontal during the measurement.
- Protect the inclinometers from direct sunlight before and during the measurements by putting the plastic tube over it or by choosing a place in the shade.



- Switch on the inclinometer at least 15 min before the measurement.
- Organize the cable routing in such a way, that mechanical stress on the inclinometer is inhibited and that cables do not get tangled when the module is turned.

4.3.2.3 Camera setup

The camera Nikon D300 is situated 30-40 m away of the measured module in the man lift for a zenith deflectometry or on the ground for a horizon deflectometry. Sometimes a horizon deflectometry is carried out from a man lift as well, depending on the surrounding of the module.

Fix the tripod in the basket of the man lift in a stable position. For a higher security, fix a safety leash to the basket of the man lift and put the safety belt of the camera over the tripod head.

Camera and laser distance meter have to be attached to a tripod adapter plate.

Camera parameter	range	comments
ISO	200	
Aperture	Closed (highest value e.g. 22)	
Exposure mode	M	
Exposure time	Depending on illumination, preferably slightly overexposed	
Flash	Adapt flash settings to target reflectivity and distance to obtain a target brightness of 100-200	
Focus	Set to ∞	
Autofocus	off	
Image size	L	



Camera parameter	range	comments
Image Quality	Fine	
JPEG compression	Optimal quality	
White balance	sunlight	

Except for very long focal length lenses (> 200 mm), most middle or short focal length lenses show significant lens distortion.

4.3.2.4 Camera calibration

Such lenses must be pre-calibrated by means of close range photogrammetry or approaches depending on checkerboard patterns (Scaramuzza 2009; Bouquet 2010). In case of a zoom lens, the pre-calibrated focal lengths must be marked at selected for the respective set-up (SCE size, Distance SCE to camera). The photogrammetric camera model used by the software (Aicon DPA Pro) in the context for the PG evaluation and is the same as presented in (Luhmann, Robson et al. 2006). The parameters provided by the bundle adjustment software are used by several MATLAB application for spatial transformations, so it essential to work with the same mathematical camera model. This model itself reaches its limits for fish-eye optics with a focal length < 10 mm, yet the typically applied cameras are described very well. Due to chromatic aberration, IOR depends in general on the selected colour-channel of an RGB-image (Luhmann, Hastedt et al. 2006).

4.4 Data acquisition

A proper documentation is the key to a successful evaluation and meaningful results. It is highly recommended to always take notes of unusual conditions and any incidences. In particular, take notice of changing wind conditions for individual measurement points or series.

4.4.1 Safety issues

It must be paid special attention that the collector never faces to the sun (if there is no HTF circulated inside the absorber tubes) as the absorber tube could be destroyed by



concentrated radiation and the lack of heat sink.

The use of a man lift requires a special training and safety precautions (harness, helmet with chin strap) are compulsory.

4.4.2 Position of camera and man–lift

Place the man lift in Y-direction (along the absorber tube) above the centre of the collector. During data evaluation, the reflection of the man lift has to be deleted, so there is no information available in these areas. But if there is information available around the deleted areas, data can be interpolated. Thus, try to place the man lift in such a way, that the reflex of the boom of the man lift is perpendicular to the y axis.

With use of the tripod head, position the camera in a way so that:

- whole module is visible (module corners are not covered)
- Parabola vertex appears horizontally in the landscape orientated image
- arrangement in respect to y axis: optical axis of camera is perpendicular to y axis of module and incidences where the reflex of the camera is visible
- arrangement in respect to x axis: optical axis of camera incidences with the rotation axis of the module

Measurements in horizontal collector angle should not be done when the module is shading the ground (e.g. measurement in eastern horizontal collector angle in the afternoon). The shade appears very dark in the measurement photos.

In case the sun is illuminating the side of the receiver which is facing to the collector, there might be a very bright (white, blue or violet) reflex of the absorber in the measurement photos. This can occur for example in zenith angle in the very morning or evening. These reflexes should be avoided.

4.4.3 Angle range

Before starting the measurement, the motion range of the collector angle must be identified. For this purpose the collector is turned in one direction, until the absorber reflection has just left the mirror. The same procedure is executed for the other direction, and the



corresponding angle values denote the motion range.

4.4.4 Image acquisition

- Calculate the angle step (angle range divided by number of photos). Usually it is between 0.2° and 0.3° .
- Turn the module to the initial angle where the reflection of the glass envelope is almost appearing in the lower or upper part of the module.
- Take the first photo and note the collector angle with the inclinometer. The photo number and the corresponding angle have to be documented.
- Turn the module by the angle step and take the second photo with the associated collector angle.
- Proceed until the reflection of the receiver tube leaves the mirror surface.

4.4.5 Measurement of camera position

Attach the laser distance meter to the tripod head. Measure the distance to end of the vertex (FEP and REP) at least three times. During the measurement do not move or touch the laser distance meter.

4.4.6 Absorber tube position

As direct access to the steel tube is prevented by the glass envelope tube, measurement of absorber tube position is in general a two stage process. At first, the axis of the glass envelope tube is measured and then the eccentricity of absorber and glass tube is estimated from digital images. The superposition of glass envelope tube position and eccentricity gives the absolute deviation of the steel tube from the focal line.

In a photogrammetric measurement, the centre of glass envelope tube can be calculated by fitting a circle to a ring of 3D coordinates from targets attached to the circumference of the glass envelope tube. For this process as a first step, the 3D coordinates of all POI must be transformed into the design coordinate system according to section 3.8.2.

This photogrammetric approach can hardly be applied to larger numbers of SCE because it requires substantial preparation efforts. In addition, for the TARMES measurement, the effort



would be disproportional if also a complete photogrammetric measurement was carried out. A less precise but much faster approach involves the direct manual distance measurement between the glass envelope tube and the outer mirror edges with a hook rod, in order to obtain lateral deviations. Vertical deviations are derived from photos for the supports, which indicate the tilting of the supports. These pictures have to be taken immediately after the TARMES measurement, as it may change in time with changing HTF temperatures.

To obtain the eccentricity of the steel absorber tube relative to the glass envelope tube, digital images showing close-ups of the HCE can be used to obtain the absorber tube position. Therefore, images are taken along the optical axis and perpendicular to the optical axis and vertex. The edges of the steel and glass tube are calculated from cross sections perpendicular to the focal line. The combination of these methods yields the relative orientation between the PTC focal line and the steel tube centre axis with an accuracy of +/- 1.2 mm.

4.5 Evaluation and post-processing

4.5.1 Software

The software used for the TARMES evaluation by DLR is a proprietary MATLAB code which is not being shared. The basic steps carried out by the software during evaluation and post-processing are described hereinafter.

4.5.2 Determination of 3D setup

Precise determination of the six parameters describing the camera position and orientation has highest relevance for the measurement accuracy. The importance is based in the fact, that the camera position is involved in the final mirror-normal vector calculation (compare Figure 4), as well as in all intermediate steps of the post-processing like ortho-image creation. The distance between camera and vertex and the inclinometer data provide the camera position for each image in the local SCE coordinate system (Figure 1).

The three angles describing the orientation of the camera are obtained by minimizing the 3D residuals between projected SCE corners and those selected by the user.



4.5.3 Image rectification

In order to detect and compare absorber tube reflections from a series of images, while the SCE position within the image varies between consecutive frames, it is indispensable to rectify each image and create matrices with an aspect ratio that corresponds to actual collector aperture. Each pixel in the ortho-image matrix can be assigned to a specific location in the ideal concentrator geometry, defined by the horizontal distance from the vertex (X-axis), the position along the vertex (Y-axis), and the height (Z-axis). Same locations of the mirror surface appear at identical positions in the ortho-image matrix, so that subsequent results of the image processing can be combined in a single matrix.

The terms ortho-photos or ortho-images (Habib, Kim et al. 2007) is mainly used in aerial imagery and describes geometrically corrected raw images by considering topographic relief, lens distortion, and camera tilt. In the present application, spatial information of the 3D-setup (EOR relative to collector module) is used to calculate the 2D transformation from the raw-image to the ortho-image. In a first approximation, this is a projective transformation, but the consideration of lens distortion (IOR) and the curved surface requires a pixel-wise transformation, which is described by a look-up table assigning to every pixel in the raw image exactly one pixel in the target matrix.

For that purpose, an ideal collector grid is created with spatial resolution (typically 6 mm/pixel) according to the actual image resolution. This grid is projected into the image using the EOR and IOR from the photogrammetric evaluation, so that pixel locations in the raw image can be assigned to each grid point of the ideal collector. Grey-values of each colour-channel of these pixels are transferred to the corresponding position in the ortho-image matrix. Next-neighbour interpolation is used to smooth the result.

4.5.4 Detection of absorber tube reflection

Due to ortho-image creation, the reflex position is found within the surface of the ideal parabolic trough, so that the detection of an absorber tube edge reflection can be assigned to a 3D position.

Basically, the detection of the (dark) absorber tube reflection in front of the (bright) sky background is performed by global thresholding (Otsu 1975). A binary image (TRUE: Absorber tube reflection, FALSE: Sky) is created by segmenting the grey-scale image, where



all pixel with grey-values above the global threshold are set to TRUE while all other pixel are set to zero. The edges of the binary image represent the required coordinates for mirror shape calculation. This straightforward approach (global thresholding, edges of binary image represent absorber tube reflection edges) delivers good results, when the mirrors haven been cleaned prior to the measurement and data acquisition is carried out under overcast sky conditions. However, the conditions in the solar field before and during data acquisition often cause unfavourable data quality that prevents the use of global thresholding without further corrective measures:

- Inhomogeneous background: due to the curvature of the mirror, a wide section of the sky is visible in the mirror. Intensity variations within that background can be caused by bright or dark clouds. But even under clear sky conditions, there is a significant intensity variation between bright areas as the horizon- and circumsolar region and dark areas of the celestial dome. The scale of this variation, in combination with other problematic conditions, may result in weak contrast between the tube reflection and dark areas of the clear sky.
- Inhomogeneous illumination: Optimal raw data is obtained under over overcast sky conditions. As CSP plants are preferably installed in regions with high DNI, the challenge is to cope with phenomena arising from specular reflection causes by direct radiation from the sun, like shadows, scattering, and specular reflections on the absorber tube.
- Soiling: Dust on the mirror diminishes the overall contrast and tends to enhance the effect of inhomogeneous illumination.

4.6 Calculation of mirror shape

This step is carried out according to the methodology depicted in Figure 4, or with one of the other DO methods presented in Section 2.2.

4.7 Data format

The results are in general provided as two-dimensionally high resolved SDX maps. Slope deviations are expressed in *milli-radians* [mrad]. Those maps could be saved as ASCII files with rather large storage requirement. It is more advisable to use a more efficient data format like Matlab workspaces (.mat).





5 Protocol for characterization of complete solar concentrators with airborne deflectometry

Optical measurement techniques are the first choice to determine the geometric, optical, and also some thermal properties of PTC solar fields. The application of UAVs is a natural consequence to overcome restrictions arising from state of the art, ground based data acquisition with stationary cameras. Going airborne offers the possibility to automatically obtain high resolution information on the concentrator geometry for large fractions or even the entire solar field with virtually negligible impact on plant operation. The current section describes briefly the implementation of DO (distant observer) characterization techniques using airborne data acquisition. The DO techniques using the absorber tube reflections offer benefits compared to scanning or pure photogrammetric approaches, because apart from the camera, no additional installations or manipulations in the solar field are required

5.1 Equipment

The main difference to ground based DO methods is the use of an UAV (Unmanned Aerial Vehicle) and a suitable payload (camera)

Item	Description	Example
UAV	Quadcopter	Md4-1000
Camera	Resolution > 20 MP	Sony NEX-7
Auxiliary equipment	Remote control batteries & chargers ground station	



5.2 Boundary conditions

Similar boundary conditions as described in Section 4.2 apply. Differences are presented in the following table

Parameter	Range	comments
Ambient light	Daylight, ideally cloudy sky.	
Wind	< 6 m/s	Restrictions for flight safety
Space requirements	Flat area for take-off and landing Flight height is regulated by national authorities	
Collector status: Elevation angle	90° +/- 5° for zenith measurements	

Table 4: Boundary conditions for airborne deflectometry

5.3 Preparation and data acquisition

In order to provide reproducible and accurate camera positions relative to the SCE, automatic GPS guided Waypoint flight routes are indispensable, The manual navigation of the UAV via Remote Control is only required for take-off and landing.

The design of the Waypoint route depends on the desired results, and the collector and solar field design. Figure 9 provides a typical flight route used for simultaneous measurement of absorber tube position and mirror shape.

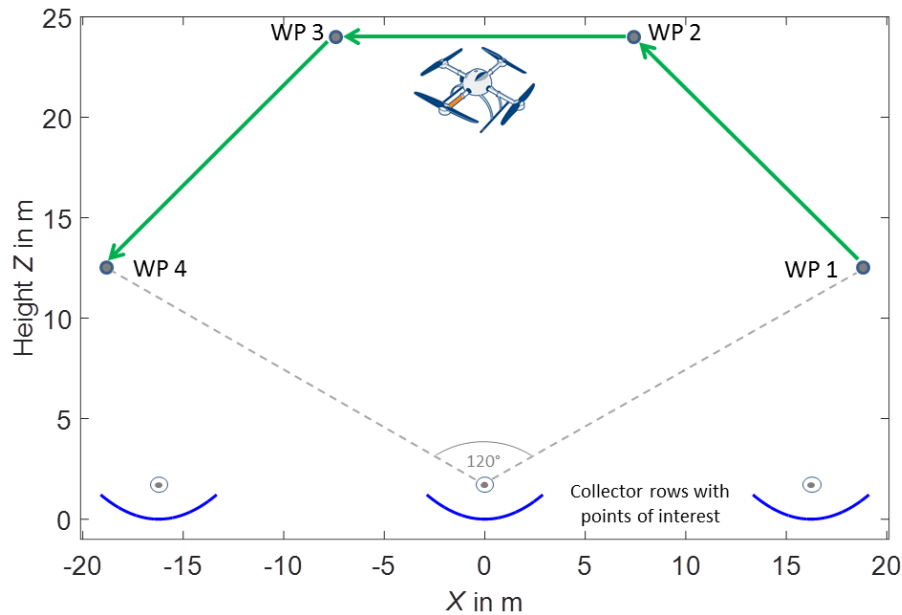


Figure 9: Cross section perpendicular to the focal line showing the parabolic mirror with the Waypoints of each SCE flyover. Images relevant for the mirror shape are taken along WP2WP3, while additional images for the absorber tube positioning are taken along WP1WP2 and WP3WP4.

The measurement process consists mainly out of preparatory steps. The following list describes the order of relevant steps of the data acquisition:

- Determination SCE-, SCA-, and solar field geometry from drawings
- Get latitude, longitude, and altitude of the drive pylon selected as origin of the local Cartesian coordinate system by using appropriate web-tools. GNSS measurements in the solar field are prone to systematic errors caused by shading of satellites and the influence on the metal structure, so that using the coordinates from <http://www.geoplaner.com/> or similar is much more reliable.
- Timing of the data acquisition must consider solar position and orientation of the solar field to avoid specular reflections of solar radiation disturbing the absorber tube detection.
- Create WP route with and cross check with appropriate software
- Transfer WP to the UAV
- Before take-off: it is mandatory to follow the checklist provided by the UAV manufacturer covering all safety issues
- Switch the UAV flight mode to automatic WP navigation in order to initiate image



acquisition according to settings

- After finishing the WP route, the UAV returns automatically to the take-off position. Landing is done manually.

5.4 Evaluation and post-processing

The evolution of the airborne data follows in general the methodology of ground based measurements.

Spatial attention must be paid to the accurate determination of the camera position relative to the SCE. A well-proven approach is the use of close range photogrammetry (Prahl, Stanicki et al. 2013)

6 Measurement of solar concentrators with laser trackers

Laser trackers can be used to determine the 3D model of solar concentrators as an alternative of Photogrammetry methodology; and use it for computing figures included on section 1.3 by ray tracing software afterwards.

The current section describes briefly the use of laser trackers characterization techniques.

6.1 Equipment

The only needed equipment for this methodology is a laser trackers capable to scan objects and 3D surfaces. As an example, Table 5 below shows technical specifications of one laser scanner model used for geometrical assessment of solar concentrators.

Wavelength	808nm
Laser Class	Class 1 laser (IEC60825:2014)
Ray Divergence	0,2 mrad



Ray Diameter on frontal window	≤ 2,8 mm
Measurement range	0,4-120 m
Angular accuracy	8"
3D accuracy	3mm (@50m)
Noise (for white targets)	0,7mm (@50m)

Table 5: Technical characteristics of the P20 ScanStation used for building the reflecting heliostat surface 3_D model.

6.2 Boundary conditions

Similar boundary conditions as described in Section 4.2 apply. Differences are presented in the following table

Parameter	Range	comments
Ambient light	Daylight, ideally cloudy sky.	
Wind	< 4 m/s	
Space requirements	Minimum space required for direct vision of the concentrator at normal incidence (+/- 10°)	
Collector status:	Reflective surfaces must be white coated to avoid laser reflection	

Table 6: Boundary conditions for laser tracker methodology

6.3 Preparation and data acquisition

The measurement process consists mainly on scanning the concentrator with the laser tracker at a required distance from the concentrator. 3D model is exported afterwards in 3D coordinates table at the required resolution (up to 0.1mm).



6.4 Evaluation and post-processing

Evaluation of the laser tracker data is quite similar to the photogrammetry post-processing. A well-proven approach is the use of close range photogrammetry

7 References

- Bendt, P., A. Rabl, et al. (1979). Optical analysis and optimization of line focus solar collectors. Retrieved 2015.03.24 from: www.nrel.gov/docs/legosti/old/092.pdf, Solar Energy Research Institute, Golden, Colorado (USA).<http://www.nrel.gov/docs/legosti/old/092.pdf>
- Diver, R. B. and T. A. Moss (2007). "Practical field alignment of parabolic trough solar concentrators." *Journal of Solar Energy Engineering* **129**(2): 153-159.
- Habib, A. F., E.-M. Kim, et al. (2007). "New methodologies for true orthophoto generation." *Photogrammetric Engineering & Remote Sensing* **73**(1): 25-36.
- Heimsath, A., W. Platzer, et al. (2008). Characterization of optical components for linear Fresnel collectors by fringe reflection method. Proceedings of the 14th SolarPACES Conference, 4. - 7. March 2008, Las Vegas, USA.
- Heinz, B. (2005). Entwicklung eines optischen Messsystems zur Bestimmung der Steigungsfehler von Parabolspiegeln solarthermischer Kraftwerke, TU München.
- Janotte, N., G. Feckler, et al. (2014). "Dynamic performance evaluation of the HelioTrough} collector demonstration loop--towards a new benchmark in parabolic trough qualification." *Energy Procedia* **49**: 109-117.
- King, P., P. Comley, et al. (2014). "Parabolic trough surface form mapping using photogrammetry and its validation with a large Coordinate Measuring Machine." *Energy Procedia* **49**: 118-125.
- Knauer, M. C., J. Kaminski, et al. (2004). Phase measuring deflectometry: a new approach to measure specular free-form surfaces. Photonics Europe.
- Lewandowski, A. and A. Gray (2010). Video Scanning Hartmann Optical Tester (VSHOT) Uncertainty Analysis. Proceedings of the 16thth SolarPACES Conference, 21. - 24. September 2010, Perpignan, France.



Luhmann, T., H. Hastedt, et al. (2006). Modelling of chromatic aberration for high precision photogrammetry. Commission V Symp. on Image Engineering and Vision Metrology, Proc. ISPRS.

Luhmann, T., S. Robson, et al. (2006). Close range photogrammetry: Principles, Techniques and Applications, Whittles Publishing.

Lüpfert, E. and S. Ulmer (2009). Solar trough mirror shape specifications. Proceedings of the 15th SolarPACES Conference, 15. - 18. September 2009, Berlin, Germany.

Montecchi, M., A. Benedetti, et al. (2010). Optical Alignment of Parabolic Trough Modules. Proceedings of the 16th SolarPACES Conference, 21. - 24. September 2010, Perpignan, France.

Otsu, N. (1975). "A threshold selection method from gray-level histograms." *Automatica* **11**(285-296): 23-27.

Owkes, J. K. (2012). An Optical Characterization Technique for Parabolic Trough Solar Collectors Using Images of the Absorber Reflection, University of Colorado.

Pottler, K., E. Lüpfert, et al. (2004). Photogrammetry: A powerful tool for geometric analysis of solar concentrators and their components. ASME 2004 International Solar Energy Conference.

Pottler, K., S. Ulmer, et al. (2014). "Ensuring Performance by Geometric Quality Control and Specifications for Parabolic Trough Solar Fields." *Energy Procedia* **49**(0): 2170-2179.

Prahl, C., B. Stanicki, et al. (2013). "Airborne shape measurement of parabolic trough collector fields." *Solar Energy* **91**(0): 68-78.

Shortis, M. and G. Johnston (1997). "Photogrammetry: an available surface characterization tool for solar concentrators, part II: assessment of surfaces." *Journal of Solar Energy Engineering* **119**(4): 286-291.

Stynes, J. K. and B. Ihas (2012). Slope error measurement tool for solar parabolic trough collectors. World Renewable Energy Forum, Denver, Colorado.

Ulmer, S., B. Heinz, et al. (2006). Slope error measurements of parabolic troughs using the reflected image of the absorber tube. Proceedings of the 13th SolarPACES Conference, June 2006, Seville, Spain.

Ulmer, S., B. Heinz, et al. (2009). "Slope error measurements of parabolic troughs using the



- reflected image of the absorber tube." *Journal of Solar Energy Engineering* **131**(1): 011014.
- Ulmer, S., P. Heller, et al. (2008). "Slope measurements of parabolic dish concentrators using color-coded targets." *Journal of Solar Energy Engineering* **130**(1): 011015.
- Ulmer, S., T. März, et al. (2011). "Automated high resolution measurement of heliostat slope errors." *Solar Energy* **85**(4): 681-687.
- Ulmer, S., K. Pottler, et al. (2007). *Measurement Techniques for the Optical Quality Assessment of Parabolic Trough Collector Fields in Commercial Solar Power Plants. Proceedings of ES2007.*
- Ulmer, S., C. Weber, et al. (2012). *High-resolution measurement system for parabolic trough concentrator modules in series production. Proceedings of the 18th SolarPACES Conference, 11. - 14. September 2012, Marrakech, Morocco.*
- Weber, C., S. Ulmer, et al. (2014). "Enhancements in high-resolution slope deviation measurement of solar concentrator mirrors." *Energy Procedia* **49**: 2231-2240.
- Wendelin, T., K. May, et al. (2006). *Video scanning hartmann optical testing of state-of-the-art parabolic trough concentrators. ASME 2006 International Solar Energy Conference.*
- Wood, R. (1981). *Distant observer techniques for verification of solar concentrator optical geometry, Technical Report UCRL-53220 and Lawrence Livermore National Laboratory.*
- WorldBank (2010). *MENA Assessment of the Local Manufacturing Potential for Concentrated Solar Power (CSP) Projects.* <http://www.cspworld.org/resources/mena-assessment-local-manufacturing-potential-concentrated-solar-power-csp-projects>, World Bank Group.
- Xiao, J., X. Wei, et al. (2012). "A review of available methods for surface shape measurement of solar concentrator in solar thermal power applications." *Renewable and Sustainable Energy Reviews* **16**(5): 2539 - 2544.